Polypyrrole–Multiwalled Carbon Nanotubes Composites as Immobilizing Matrices of Ascorbate Oxidase for the Facile Fabrication of an Amperometric Vitamin C Biosensor

Dong Li,[1,2] Yangping Wen,[1,2] Haohua He,[1] Jingkun Xu,[2] Ming Liu,[1,2] Ruirui Yue[2]

[1]*Key Laboratory of Crop Physiology, Ecology and Genetic Breeding, Ministry of Education, Key Laboratory of Physiology, Ecology and Cultivation of Double Cropping Rice, Ministry of Agriculture, Jiangxi Agricultural University, Nanchang 330045, China*
[2]*Jiangxi Key Laboratory of Organic Chemistry, Jiangxi Science and Technology Normal University, Nanchang 330013, China*

Received 17 May 2011; accepted 21 November 2011
DOI 10.1002/app.36526
Published online in Wiley Online Library (wileyonlinelibrary.com).

ABSTRACT: An amperometric vitamin C biosensor was facilely fabricated by the immobilization of ascorbate oxidase (AO) on polypyrrole (PPy)–multiwalled carbon nanotubes (MWCNTs) composites with a one-step electrodeposition technique in a 0.05*M* phosphate buffer solution (pH 6.5). The cyclic voltammetry, IR spectral analysis, electrochemical impedance spectroscopy, and scanning electron microscopy measurements indicated that AO was successfully immobilized on the PPy–MWCNT composites. The optimization of the biosensor parameters, including the working potential, pH, and temperature, was investigated in detail. The proposed biosensor showed a linear range of 5×10^{-5} to 2×10^{-2} *M* with a detection limit of 0.3 μ*M*, a sensitivity of 25.9 mA mM^{-1} cm^{-2}, and a current response time less than 20 s under the optimized conditions. The apparent Michaelis–Menten constant together with the apparent activation energy indicated that the proposed biosensor exhibited a high bioaffinity and a good enzyme activity. In addition, the biosensor also showed good operational and storage stabilities. © 2012 Wiley Periodicals, Inc. J Appl Polym Sci 000: 000–000, 2012

Key words: conducting polymers; carbon nanotubes; electrochemistry; enzymes; sensors

INTRODUCTION

Vitamin C (VC), one of the most important vitamins for human beings, cannot be synthesized by human beings and must be obtained in the daily diet. Beyond its function in collagen formation, VC is also known to increase the absorption of inorganic iron, to have essential roles in the metabolism of folic acid and some amino acids and hormones, and to act as an antioxidant.[1] It is, therefore, very important to develop a quick and effective method for the detection of VC in fruits, vegetables, grain crops, and drinks. Traditional methods, such as titrimetric, chromatographic, and spectrophotometric methods, have some disadvantages, including complex sample pretreatment procedures, high manufacturing costs, time-consuming manipulations, and low sensitivities.[2–4] Hence, a need has arisen for a fast, sensitive, and inexpensive method to detect VC, and a substitution of analytical methods with enzyme-based biosensors would be very significant.

Because of their high sensitivity, fast response, simplicity, and easy miniaturization, a variety of ascorbate oxidase (AO) based biosensors were fabricated by different materials as immobilization matrices of enzymes for the detection of VC.[5–13] Of these materials, intrinsic conducting polymers (ICPs), which are unique in their ability to act as both mediators and immobilization matrices for enzyme retention, have attracted widespread attention in the

The first two authors contributed equally to this work.

Correspondence to: H. He (hhhua64@163.com) or J. Xu (xujingkun@tsinghua.org.cn).

Contract grant sponsor: National Natural Science Foundation of China; contract grant number: 50963002 and 51073074.

Contract grant sponsor: Key Projects in the National Science & Technology Pillar Program in the Eleventh Five-Year Plan Period; contract grant number: 2006BAD02A04 and 2006BAD01A01.

Contract grant sponsor: Key Laboratory of Photochemical Conversion and Optoelectronic Materials, Technical Institute of Physics and Chemistry, Chinese Academy of Sciences, Jiangxi Provincial Department of Science and Technology; contract grant number: 2006BAD01A01-2-5.

Contract grant sponsor: Jiangxi Provincial Department of Education; contract grant number: 2006BAD01A01-2-5.

Contract grant sponsor: Natural Science Foundation of Jiangxi Province; contract grant number: 2010GZH0041.

Contract grant sponsor: Jiangxi Provincial Innovation Fund of Postgraduates; contract grant number: YC10A063.

fabrication of efficient biosensors. ICPs, such as polyaniline, polypyrrole (PPy), and poly(3,4-ethylenedioxythiophene), have been considered as electrode materials for the fabrication of AO-based biosensors in previous studies.[7,8,12,13] Among these ICPs, PPy plays a leading role because of its superior properties, which include good solubility in aqueous solutions, high electrical conductivity, low material cost, good environmental stability, and particularly, a relative ease of synthesis and good biocompatibility.[14,15] For these reasons, PPy is more suitable for the immobilization of enzymes in the fields of biosensors than other ICPs. However, the main drawback of enzyme-based biosensors based on PPy matrices is low mechanical properties;[16] this raises a challenge for practical application. To solve this problem and enhance the biosensing performance, various PPy composites have been developed.[17–19] In particular, multiwalled carbon nanotubes (MWCNTs) have gained considerable attention in recent years because of their significant mechanical properties, high surface area, and high electrical conductivity.[20–26] Therefore, MWCNTs have been used to facilitate the immobilization of enzymes and the development of efficient biosensors.[27–31] Moreover, the presence of MWCNTs in enzyme-based biosensors is beneficial for improving the stability of the biosensors.[32,33] Therefore, it is a good idea to synthesize PPy composites with MWCNTs, which can be used as the matrices for the immobilization of AO. As reported previously, PPy–MWCNT composites have attracted considerable attention because not only can the introduction of MWCNTs improve the conductivity and mechanical properties of composites, but the composites also possess the properties of the individual components with a synergistic effect.[34–38] However, there has been no report on the electrochemical immobilization of AO on the PPy–MWCNT composites for the fabrication of amperometric VC biosensors.

In this study, an amperometric VC biosensor was fabricated successfully by the immobilization of AO in PPy–MWCNT composites. In addition, the electrochemical properties and surface morphologies of the PPy–MWCNT composites and enzyme electrodes were studied by cyclic voltammetry, electrochemical impedance spectroscopy (EIS), IR spectral analysis, and scanning electron microscopy (SEM). The optimal parameters and performance analysis of the proposed biosensor were investigated in detail.

EXPERIMENTAL

Chemicals

AO (EC 1.10.3.3, 162 U mg^{-1}, from *Cucurbita* sp.) and pyrrole (Py) were purchased from Sigma-Aldrich (Shanghai, China). Lithium perchlorate trihydrate ($LiClO_4 \cdot 3H_2O$), disodium hydrogen phosphate dodecahydrate ($Na_2HPO_4 \cdot 12H_2O$), and sodium dihydrogen phosphate dihydrate ($NaH_2PO_4 \cdot 2H_2O$) were purchased from Sinopharm Chemical Reagent Co., Ltd (Shanghai, China). A 0.05 M phosphate buffer solution (PBS; pH 6.5) was made from a 0.05 M Na_2HPO_4 solution and a 0.05*M* NaH_2PO_4 solution. VC was purchased from Bio Basic, Inc (Toronto, Canada). All of these chemicals were analytical grade and were used as received without further purification. Dispersed MWCNT solutions were purchased from Chengdu Institute of Organic Chemistry, Chinese Academy of Sciences (MWCNT content = 4.39 wt %, o.d. = 50–100 nm, length = 5–15 μm). All solutions were prepared with deionized water as a solvent.

Electrochemical experiments

Electrochemical polymerization and measurements were performed in a one-compartment cell. A platinum disc electrode with a diameter of 0.3 cm was the working electrode, a stainless steel wire with a diameter of 1 mm was used as the counter electrode, and the reference electrode was a saturated calomel electrode (SCE). The electrodes were placed 0.5 cm apart during the experiments. Before each experiment, the stainless steel wire was carefully polished with abrasive paper (1500 mesh). The platinum disc electrode was polished with alumina (Al_2O_3; 0.05 μm). Then, the stainless steel wire and platinum disc electrode were rinsed sequentially by ultrasonic cleaning in acetone, ethanol, and deionized water for 5 min and dried in air. All solutions (except for the solutions containing VC) were deoxygenated by bubbling with dry argon for 20 min before each experiment. All of the experiments (except for those containing VC) were performed under a slight argon overpressure. Unless otherwise stated, the temperature was kept at 25°C.

Construction of the enzyme electrodes

The optimization of the PPy–MWCNT composites was studied by an electrochemistry method. For the construction of the enzyme electrode, the enzyme composite modified electrodes were prepared in 0.05*M* PBS (pH 6.5) containing 0.1 mg/mL AO, 0.1*M* Py, and a mass ratio of Py to MWCNTs of 5 : 1 by a one-step electrosynthesis on the surface of the working electrode. The PPy–MWCNT composites and PPy–MWCNT–AO composites was rinsed repeatedly with PBS (pH 6.5) to remove loosely bound enzyme, the electrolyte, and the monomer from the surface of the electrode. The fabricating process of the PPy–MWCNT–AO composites electrode is illustrated in Scheme 1.

Apparatus

All electrochemical experiments were performed with a potentiostat–galvanostat (model 263A, EG&G

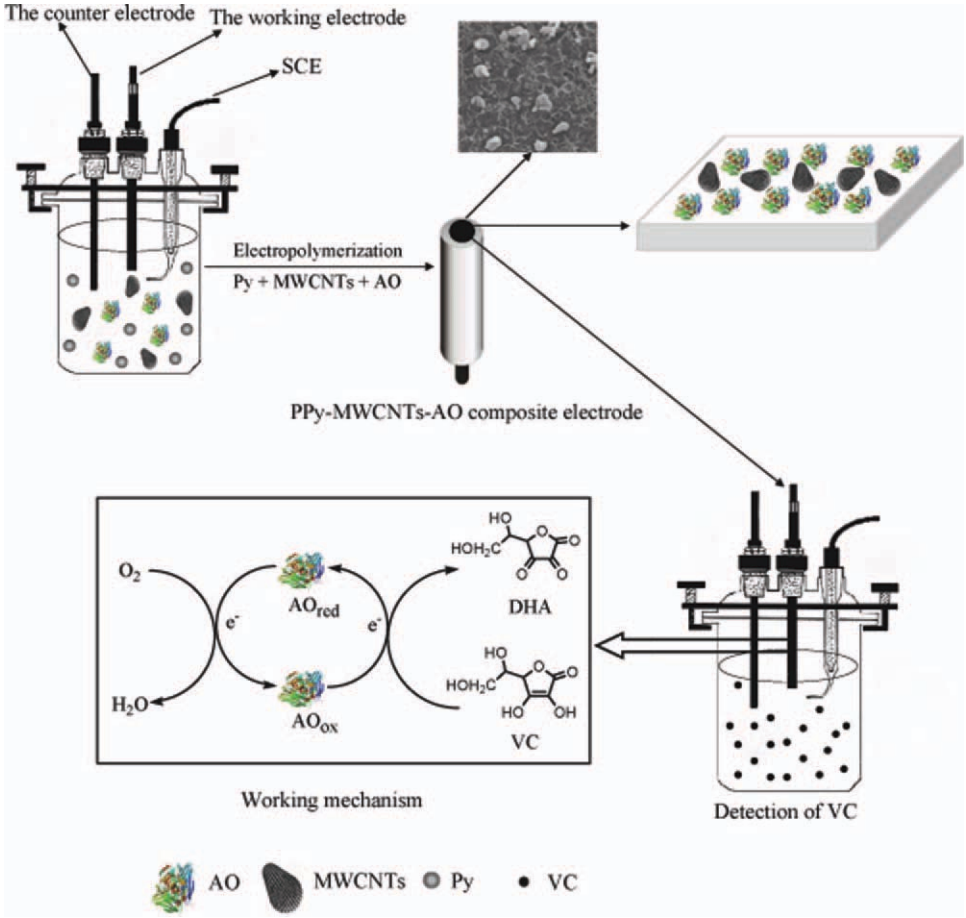

Scheme 1 Fabricated process and working mechanism of the PPy–MWCNT–AO composites electrode. [Color figure can be viewed in the online issue, which is available at wileyonlinelibrary.com.]

Princeton Applied Research, Berwyn, United States). SEM measurements were taken with a Hitachi S-3000N scanning electron microscope (Hitachi Limited, Tokyo, Japan). The pH value was measured with a Delta 320 pH meter (Mettler-Toledo Instruments, Shanghai, China). The temperature was controlled with a type HHS thermostat. IR spectra were recorded with a Bruker Vertex 70 Fourier transform infrared (FTIR) spectrometer with KBr pellets (Bruker Optik GmbH, Ettlingen, Germany). EIS was recorded with an Autolab Frequency Response Analyzer System (AUT30, FRA2-Autolab, Echemie, BV, Utrecht, Holland) in the frequency range from 100 kHz down to 10 mHz with an alternating voltage amplitude of 10 mV.

RESULTS AND DISCUSSION

Electrosynthesis of the composites and enzyme electrodes

The successive cyclic voltammograms (CVs) during the formation of the PPy films, PPy–MWCNT composites, and PPy–MWCNT–AO composites in 0.05*M* PBS (pH 6.5) containing 0.1*M* $LiClO_4$ are shown in Figure 1. As can be seen from Figure 1, the CVs exhibited similar characteristics. During the CV scan, the composites were formed gradually and adhered strongly to the surface of working electrode. The increase in the redox wave current densities implied that the amount of the polymer on the surface of electrode increased.

The redox wave current densities of the PPy–MWCNT composites [Fig. 1(B–E)] were much higher than that of the pure PPy films [Fig. 1(A)]. This was mainly because the introduction of MWCNTs might have promoted a faster charge transfer between the composites and the electrolytes, which made the composites possess a higher conductivity compared with the pure PPy films from the following charge-transfer resistance (R_{ct}). Moreover, the increase of the redox wave current densities might imply that the MWCNTs were incorporated into the PPy films. In addition, the PPy–MWCNT composites were black in color. However, as observed in this study under similar electrodeposition conditions, the PPy films were blue. Clearly, the black color of the composites was due to the presence of MWCNTs. The PPy films were very weak mechanically and could

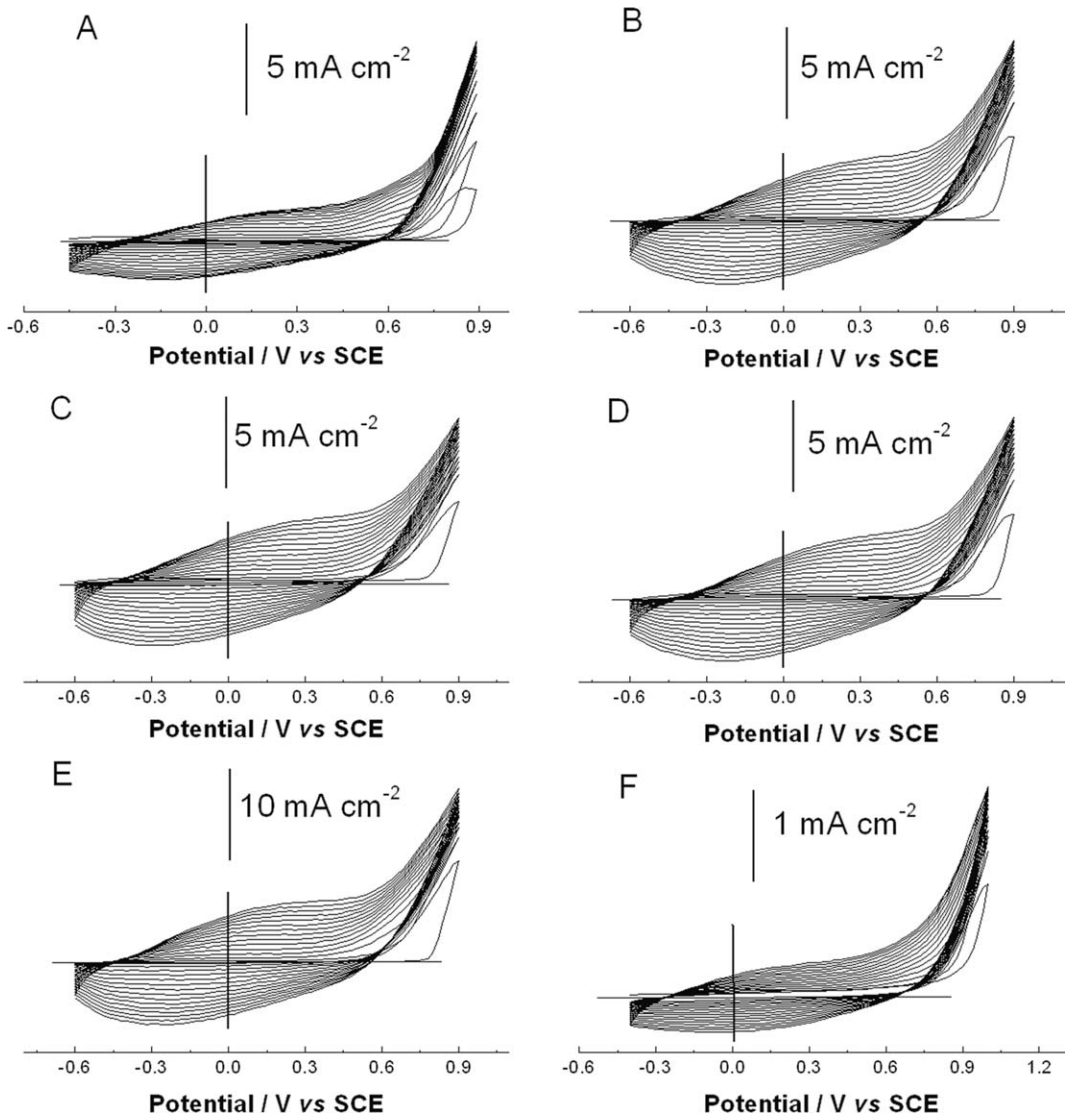

Figure 1 CVs of Py in 0.1*M* $LiClO_4$ + 0.05*M* PBS (pH 6.5) containing (A) Py (0.1*M*) and different mass ratios of Py to MWCNTs [(B) 5 : 1, (C) 2 : 1, (D) 1 : 2, and (E) 1 : 5] and (F) a mass ratio of Py to MWCNTs = 5 : 1 + AO, respectively (potential scan rate = 100 mV/s).

easily fall off if not handled with care, whereas the PPy–MWCNT composites were not shed easily from the electrode.[39] This result suggests that the PPy–MWCNT composites possessed mechanical integrity, which would be beneficial to the improvement of the stability of AO-based biosensors.

To gain a deeper insight into the electrochemical and environmental stability of the PPy–MWCNT composites, the electrochemical behaviors of these eletrochemically deposited composites were studied in monomer-free electrolyte solutions (Fig. 2). All of the steady-state CVs showed broad anodic and cathodic peaks, and the peak current densities were all proportional to the potential scan rate [Fig. 2(A–D), insert]; this indicated reversible redox behavior in the composites. Furthermore, the anodic and cathodic peak potentials of the composites were independent of the scan rates; this suggested that the redox reactions were both reversible. These films could be cycled repeatedly between the conducting (oxidized) and insulating (neutral) states without significant decomposition of the material; this indicated a high structural stability in the composites. In addition, the two curves of the anodic and cathodic peak current densities in the insert of Figure 2(A) almost overlapped; this indicated better reversible redox behavior and higher structural stability in the PPy–MWCNT composites when the mass ratio of Py to MWCNTs was 5 : 1 in comparison with the insert of Figure 2(B–D). Hence, a mass ratio of Py to MWCNTs of 5 : 1 was selected in the subsequent experiments for the immobilization of AO molecules.

The electrodeposition method has been used as an effective technique for the immobilization of

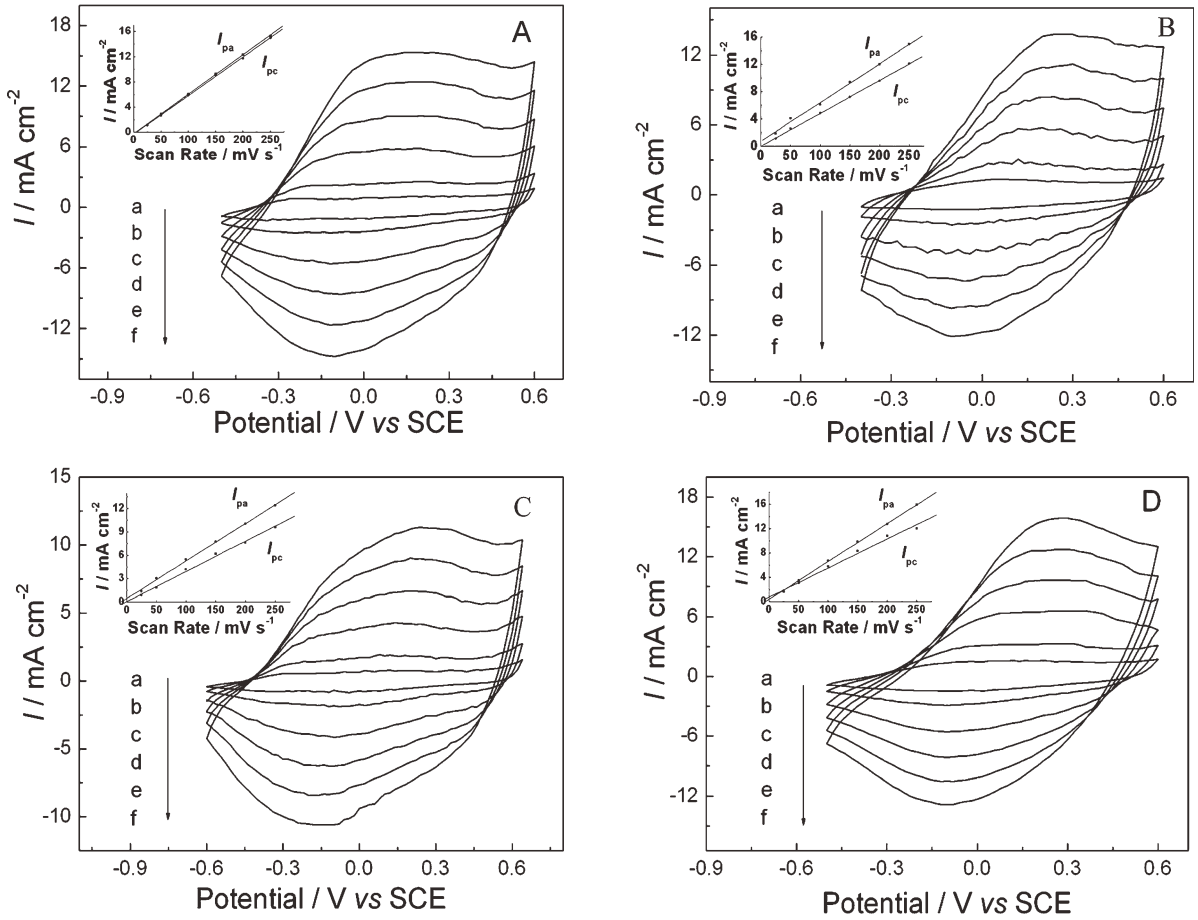

Figure 2 CVs of the PPy–MWCNT composites in monomer-free electrolyte at potential scan rates of (a) 25, (b) 50, (c) 100, (d) 150, (e) 200, and (f) 250 mV/s. The PPy–MWCNT composites were electrosynthesized in 0.05 PBS (pH 6.5) + 0.1*M* $LiClO_4$ containing different mass ratios of Py to MWCNTs [(A) 5 : 1, (B) 2 : 1, (C) 1 : 2, and (D) 1 : 5] at a constant potential of 1.0 V versus SCE. Inset: Plots of the redox peak current densities versus the potential scan rates.

enzymes on the surface of electrodes. AO molecules and MWCNTs were immobilized in the PPy films by the one-step electrodeposition technique [Fig. 1(F)]. The redox wave current densities of the PPy–MWCNT composites in the presence of AO [Fig. 1(F)] were much lower than that in the absence of AO [Fig. 1(B)]. There were two possible explanations for this phenomenon. One was that the molecular weight of AO (140 kDa) was so big that it held the growth space of the composites and led to an increase in the impedance of the composites. The other explanation was that the attachment of AO on the electrode surface prevented the Py monomer from quickly diffusing to the surface of electrode and, consequently, resulted in the weak electrochemical polymerization behavior of the Py monomer. Therefore, all these described results indicate that AO molecules could be immobilized in the PPy–MWCNT composites.

FTIR spectral analysis

The FTIR spectra of the as-formed PPy films, PPy–MWCNT composites, and PPy–MWCNT–AO composites are shown in Figure 3. The results were in good agreement with previous work.[40–42] The details of the band assignments of PPy are given in Table I. In Figure 3(B), a stronger absorption band was

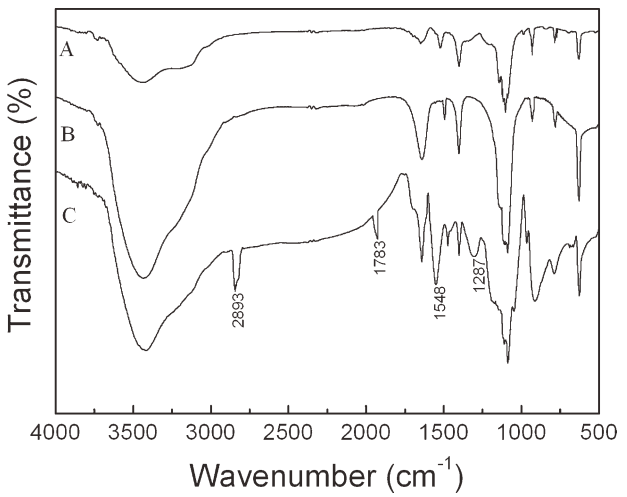

Figure 3 FTIR spectra of (A) PPy, (B) PPy–MWCNT composites, and (C) PPy–MWCNT–AO composites.

TABLE I
Assignments of the FTIR Spectra of the PPy films

Band (cm^{-1})	Assignment
3432	ν N—H
1639	ν (C=C, C—C) ring
1516	ν (C—N) ring
1369	δ C—N
1105	δ C—H
792, 983	γ C—H
632	γ C—C

ν, stretching; δ, in-plane deformation; γ, out-of-plane deformation.

observed around 1647 cm^{-1} compared with Figure 3(A); this was mainly because the presence of MWCNTs enhanced the C—C absorption peak of PPy. In addition to the characteristic peaks of the PPy–MWCNT composites in Figure 3(C), the band at about 2893 cm^{-1} was assigned to methyl and methylene asymmetric stretching vibrations of AO. In addition, there were three characteristic IR absorbance bands of AO (amides I, II, and III) that provided detailed information on the secondary structure of the polypeptide chain. The amide I band at about 1783 cm^{-1} was consistent with C=O stretching vibrations of the peptide linkage. The absorption amide II band was observed around 1548 cm^{-1}; this corresponded to the N—H stretching vibrations and C—N deformation vibration of the amide plane in the backbone of the protein. The C—H stretching vibrations and N—H deformation vibrations in the amide plane of the amide III band appeared at 1287 cm^{-1}. All of these features implied that AO existed in the composites.

EIS measurements

EIS provides an effective method for probing the electric features of surface-modified electrodes. Figure 4 shows the EIS profiles of the as-formed polymers, in which the Nyquist plots are shown with the real part (Z_{re}) on the x axis and the imaginary part (Z_{im}) on the y axis. The complex-plane plots shown in Figure 4 consist of well-defined semicircles at high frequencies with a transition to a linear part at low frequencies.[43,44] The semicircle portion at higher frequencies corresponded to the charge-transfer limited process, and the linear portion, seen at lower frequencies, may have been due to the diffusion process in the Nyquist plot of the impedance spectra. The semicircle diameter in the impedance spectrum was equal to R_{ct} at the electrode surface. The increase or decrease in the R_{ct} values exactly characterized the modification of the electrode surface. The R_{ct} values of the PPy films, PPy–MWCNT composites, and PPy–MWCNT–AO composites shown in Figure 4 were 854, 182, and 406 Ω, respectively. The R_{ct} values of the PPy–MWCNT composites [Fig. 4(B)] were much lower than those of the pure PPy films [Fig. 4(A)]. This result meant that the introduction of MWCNTs might have mediated a faster charge transfer in the parallel PPy film/solution interface and the MWCNTs/solution interface, and therefore, the conductivity of the PPy films was improved. Similarly, the R_{ct} values of the PPy–MWCNT–AO composites [Fig. 4(C)] decreased compared with those of the PPy–MWCNT composites [Fig. 4(B)]; this could be explained by the hindrance of the macromolecular structure of AO to the charge transfer. Meanwhile, it also confirmed that the AO molecules were immobilized in the composites.

In addition, Sabatani et al.[45] suggested that the change of R_{ct} is related to the apparent electrode coverage (θ), which is as follows:

$$\theta = 1 - R_{ct}^{b}/R_{ct}^{TP}$$

where R_{ct}^{b} is the charge-transfer resistance measured at the bare electrode and R_{ct}^{TP} is the charge-transfer resistance measured under the same conditions at the thiophenol-covered electrode. From this equation, it can be proven whether thiophenol was immobilized in the electrode. Similarly, the apparent electrode coverage of AO in the PPy–MWCNT electrode (θ^1) was given by

$$\theta^1 = 1 - R_{ct}^{PPy-MWCNT}/R_{ct}^{PPy-MWCNT-AO}$$

where $R_{ct}^{PPy-MWCNT}$ and $R_{ct}^{PPy-MWCNT-AO}$ are the charge-transfer resistances of the PPy–MWCNT and PPy–MWCNT–AO electrodes, respectively. The value of θ^1 was about 55.2%; this further confirmed

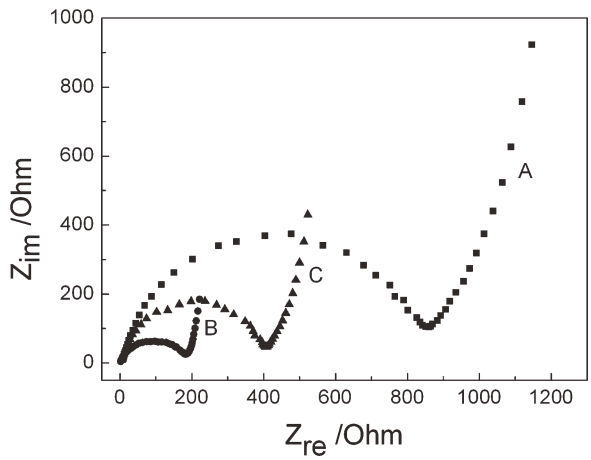

Figure 4 Impedance spectra of the (A) PPy, (B) PPy–MWCNT films, and (C) PPy–MWCNT–AO films obtained in 0.05*M* PBS (pH 6.5) containing 0.1*M* $LiClO_4$. The frequency range was 100 kHz to 10 mHz with an alternating voltage amplitude of 10 mV.

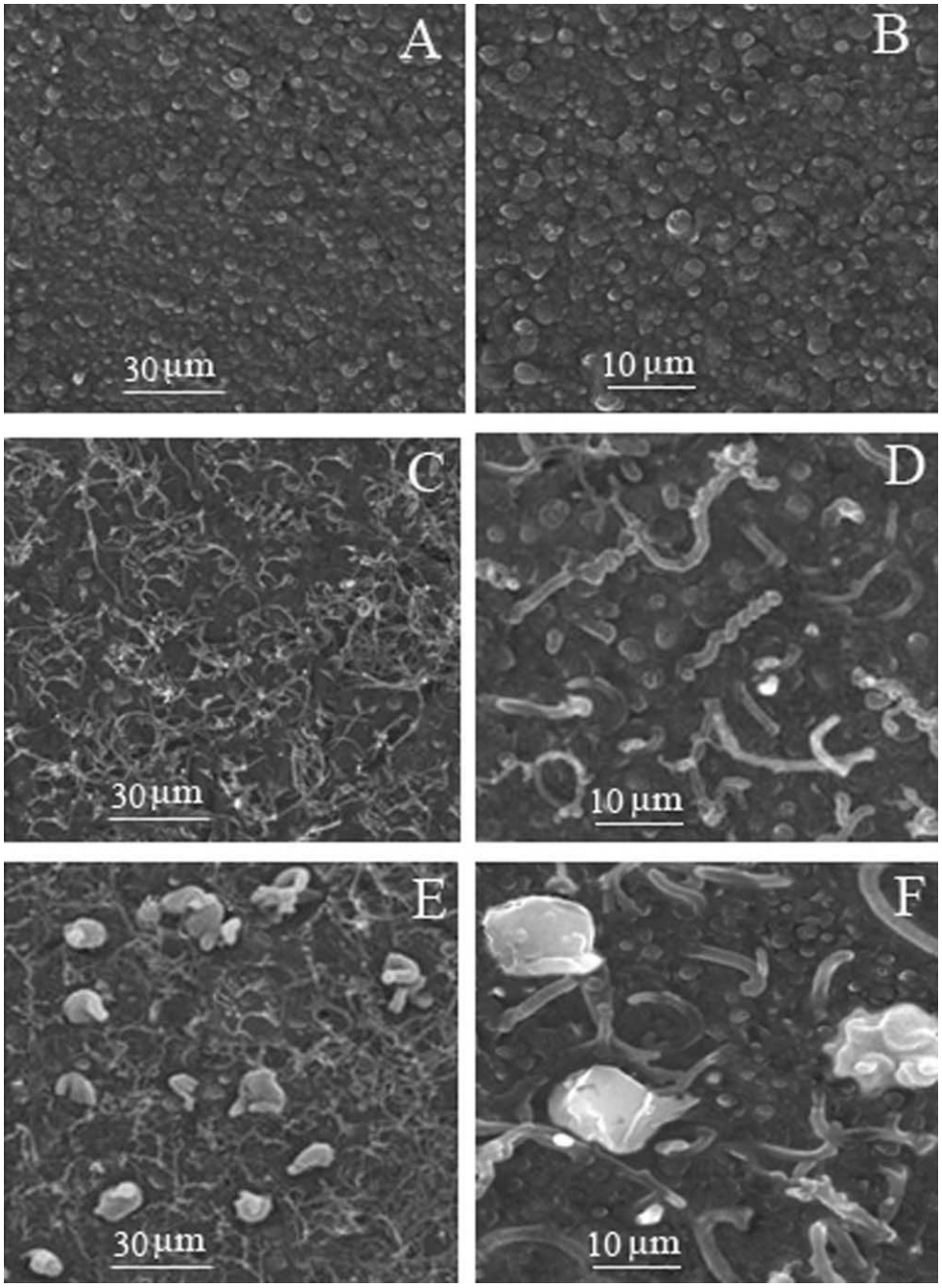

Figure 5 SEM images of the PPy films at magnifications of (A) 5000 and (B) 10,000×, the PPy–MWCNT composite films at magnifications of (C) 5000 and (D) 10,000×, and PPy–MWCNT–AO composite films at (E) 5000 and (F) 10,000×.

that the AO molecules were successfully immobilized in the PPy–MWCNT composites.

SEM images

Figure 5 shows the SEM images of the PPy films, PPy–MWCNT composites, and PPy–MWCNT–AO composites. The surface morphology of the PPy films [Fig. 5(A,B)] was in agreement with that observed in previous studies.[46] When the SEM images of the pure PPy films [Fig. 5(A,B)] and PPy–MWCNT composites [Fig. 5(C,D)] were compared, it was clear that the MWCNTs were incorporated into the PPy films during the electrodeposition. The diameter of the individual PPy–MWCNT fibrils (ca. 0.5–2 μm) was much larger than that of the corresponding MWCNTs alone (ca. 50–100 nm). This difference indicated that the MWCNTs were coated by PPy films; this may have given rise to conductive passways and led to faster electron transfer in comparison with the pure PPy films. We concluded that the PPy–MWCNT composites had a higher conductivity compared with the pure PPy films. Additionally, the MWCNT formatted 3D network serving as

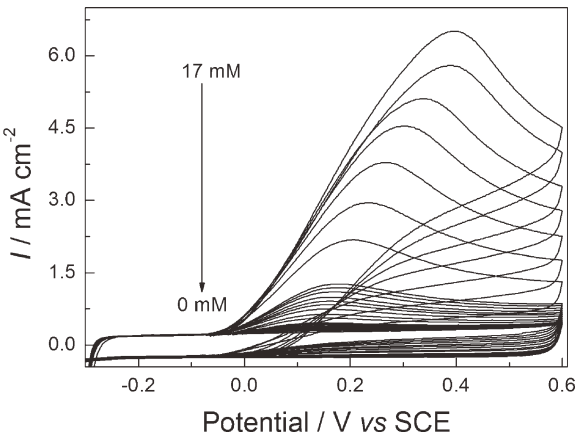

Figure 6 Electrocatalytic activity of the PPy–MWCNT–AO biosensor toward the oxidation of VC.

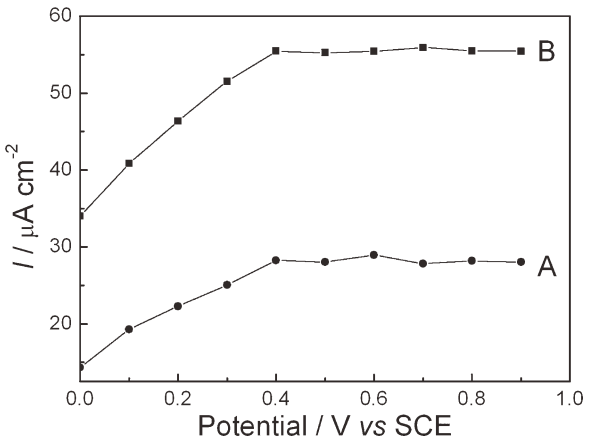

Figure 7 Effect of the working potential on the response current of the PPy–MWCNT–AO biosensor in PBS (pH 6.5) containing (A) 0.5 and (B) 1 m*M* VC at 25°C.

the backbone may have greatly improved the mechanical strength of the composites. These results were beneficial for improving the stability of the enzyme-based biosensor. The SEM images of the PPy–MWCNT–AO composites [Fig. 5(E,F)] showed big, white, and irregularly shaped AO, except for the MWCNTs; this confirmed further that the AO molecules were successfully immobilized in the PPy–MWCNT composites.

Bioelectrocatalytic performance of the biosensor

The bioelectrocatalytic activity of the proposed biosensor toward the oxidation of VC was investigated by CVs (Fig. 6). It could be seen that the bioelectrocatalytic oxidation of VC began to appear from −0.05 V and reached the maximum value at approximately 0.4 V. Moreover, the peak current density gradually increased with increasing concentrations of VC; this suggested that the proposed biosensor possessed good bioelectrocatalytic performance for the oxidation of VC. In addition, the oxidation peak potential of the proposed biosensor for the bioelectrocatalytic oxidation of VC gradually shifted to a positive potential when the concentration of VC was higher than 1 m*M*; this was ascribed to the consumption of amounts of dissolved O_2 in the surrounding enzymes.

Optimization of biosensing parameters

To optimize the parameters of the proposed biosensor, different factors influencing the response current of the proposed biosensor, such as the working potential, pH, and temperature, were investigated in detail.

The effect of the working potential on the response current of the proposed biosensor was studied, as shown in Figure 7. The response current of the biosensor quickly increased between 0 and 0.4 V. However, when the working potentials were varied from 0.4 to 0.9 V, the response current became almost constant. Additionally, the relationship between the response current and working potential showed that very little working potential dependence was present at potentials above 0.4 V. Hence, a working potential of 0.4 V was selected in subsequent experiments for the detection of VC.

The effect of pH on the response current of the proposed biosensor is shown in Figure 8. A pH value range of 5–8 was adopted in this study. The response current increased from pH 5 to 6.5 and decreased above pH 6.5. The maximum response current of the biosensor was obtained at pH 6.5. Thus, the optimum pH value was adjusted to 6.5 and used in all of the experiments discussed next.

The effect of the variation of temperature on the response current of the proposed biosensor was examined between 10 and 50°C. As illustrated in Figure 9, the response current progressively increased with increasing temperature and reached its maximum value at 35°C; it then decreased

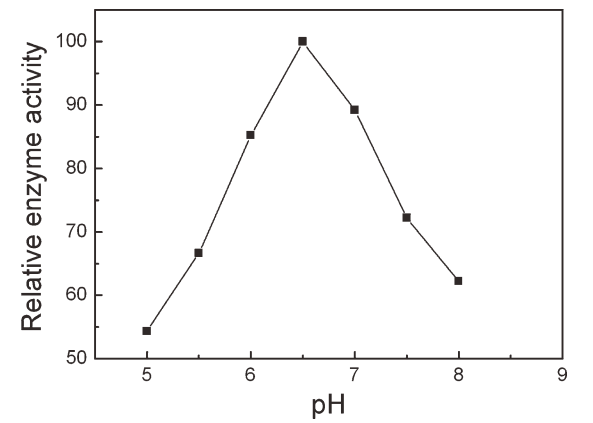

Figure 8 Effect of the pH value on the PPy–MWCNT–AO biosensor in 0.05*M* PBS containing 0.5 m*M* VC.

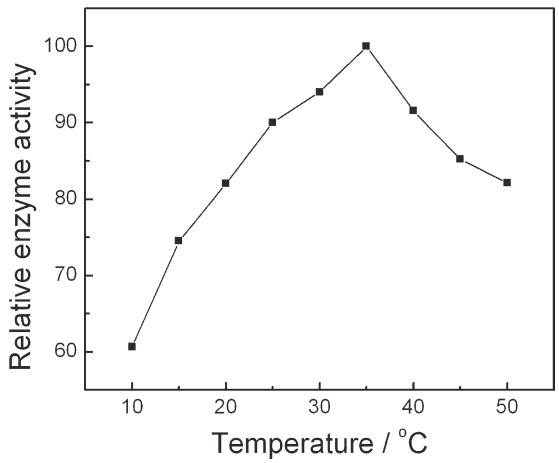

Figure 9 Effect of the temperature on the response current of the PPy–MWCNT–AO biosensor in 0.05 PBS (pH 6.5) containing 0.5 m*M* VC.

gradually. Although the biosensor showed a maximum response current at 35°C, the enzyme gradually denaturalized or became inactivate at higher temperatures. Moreover, the detection of VC in agricultural applications is usually carried out at room temperature (25°C). Hence, room temperature was chosen for the fabrication of the AO-based biosensor in all of the experiments.

Mechanism of VC detection

AO, a copper-containing homodimer enzyme, belongs to a family of oxidoreductases with a molecular weight of about 140 kDa; it contains eight copper ions and can catalyze the oxidation of VC to dehydroascorbic acid (DHA) in molecular oxygen (Scheme 1). The two substrates of the AO molecules are VC and O_2, whereas its two products are DHA and H_2O. This reaction was denoted as a double-displacement reaction mechanism,[12,47,48] which is a two-substrate reaction mechanism with two compound reactants, VC and O_2, resulting in products of DHA and H_2O. The double-displacement reaction did not occur sequentially. VC first bonded to the free-enzyme-oxidized ascorbate oxidase (AO_{ox}) and formed $VC{\cdot}AO_{ox}$; it then transformed into the reduced ascorbate oxidase (AO_{red})·DHA and next released the product DHA and formed the modifying enzyme, AO_{red}. The second substrate, O_2, also bonded to the modifying enzyme, AO_{red}, to form $O_2{\cdot}AO_{red}$, which transformed into $AO_{ox}{\cdot}H_2O$, then released another product, H_2O, and formed the free enzyme, AO_{ox}, again (Scheme 1). In the VC and O_2 reaction catalyzed by AO, the concentration of O_2 was held constant, whereas VC was varied in the as-obtained electrochemical biosensor. Therefore, freshly prepared sample solutions with different concentrations of VC were used before each measurement. Thus, the concentration of O_2 was kept constant in the air-saturated PBS in all of the experiments.

Linearity of the proposed biosensor

Figure 10 shows the current–time plots of the PPy–MWCNT–AO biosensor in 0.05*M* PBS (pH 6.5) containing VC with various concentrations at 0.4 V versus SCE for 90 s. The response current increased with increasing concentration of VC; this further indicated that the proposed biosensor had excellent bioelectrocatalytic performance for the oxidation of VC. Moreover, the biosensor showed a fast current response (within 20 s). The calibration plot (Fig. 9, inset) showed that the response current increased linearly with increasing concentration of VC in the range from 5×10^{-5} to 2×10^{-2} *M*, with a regression coefficient of 0.99. The detection limit of the biosensor was measured to be 0.3 μ*M* (Signal/Noise = 3). These results indicate that the proposed biosensor showed a better linear range and lower detection limit in comparison with the AO biosensor in our previous studies.[12,13] Additionally, the sensitivity was calculated to be 25.9 mA mM^{-1} cm^{-2} (from the slope of the initial linear part of the calibration plot).

Affinity of the biosensor

The response current of the proposed biosensor gradually deviated from the linear feature as the concentration of VC increased up to 2×10^{-2} *M*; it showed characteristics of the Michaelis–Menten kinetic mechanism (Fig. 11). The apparent Michaelis–Menten constant (K_m), which depicts the enzyme–substrate kinetics of a biosensor, could be calculated from the Lineweaver–Burke equation, as follows:

$$1/I = 1/I_{\max} + K_m/I_{\max}C$$

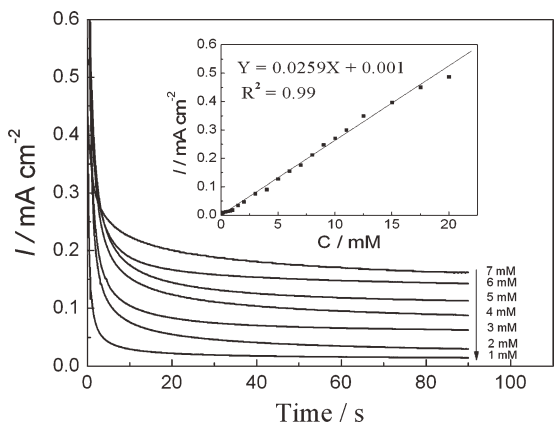

Figure 10 Current–time plots of the PPy–MWCNT–AO biosensor. Inset: calibration curve for the response current of the biosensor versus different concentrations of VC.

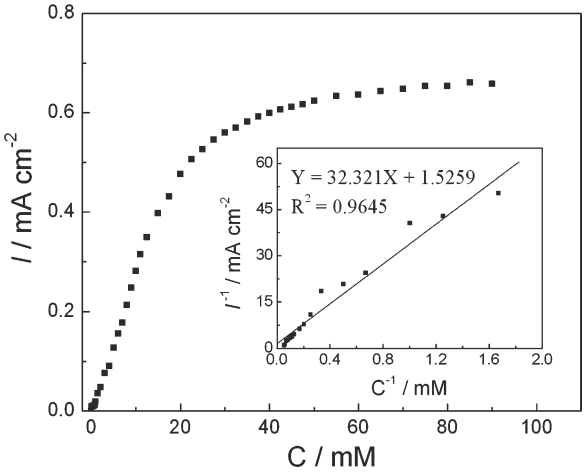

Figure 11 Relationship between the response current and the concentration. Lineweaver–Burk plots of the PPy–MWCNT–AO biosensor.

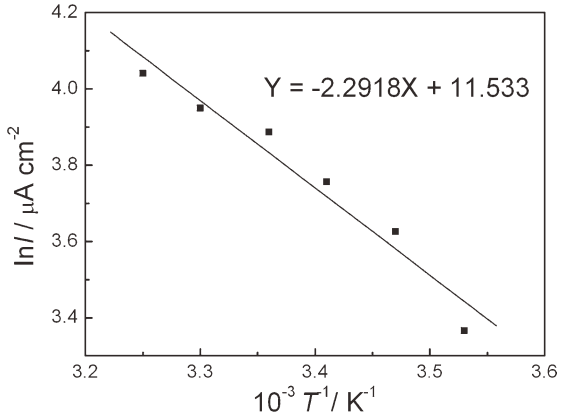

Figure 12 Determination of E_a in the plot of ln I versus $1/T$.

where C is the concentration of the substrate, I is the steady-state current, and I_{max} is the maximum current measured under substrate saturation.[49,50] The values of K_m and I_{max} were calculated to be 21.18 mM and 0.655 mA/cm^2, respectively (Fig. 11, inset). The low value of K_m implied that the AO immobilized in the PPy–MWCNT composites showed a high bioaffinity.

In addition, the dependence of the response current on the temperature could be expressed as an electrochemical version of the Arrhenius equation as follows

$$\ln I = \ln I + E_a/RT$$

where I_0 represents a collection of currents, R is the molar gas constant, T is the absolute temperature (K), and E_a is the activation energy.[51,52] The relationship between ln I versus $1/T$ was plotted, and a straight line was obtained (Fig. 12). The E_a value of the proposed biosensor was calculated to be 19.054 kJ/M, which was smaller than that reported for AO immobilized in the poly(3,4-ethylenedioxythiophene) films.[12,13] A lower value of E_a revealed that AO molecules immobilized in the PPy–MWCNT composites possessed better enzyme activity and higher bioaffinity to the substrates; this was consistent with the low value of K_m.

Operational stability of the biosensor

The operational stability of the proposed biosensor was tested in 0.05M PBS (pH 6.5), which contained equal amounts of VC; the results are presented in Figure 13. The fabrication reproducibility of six biosensors constructed independently and based on the same bare platinum disc electrode showed acceptable stability with a relative standard deviation value of 3.11%. As for one biosensor, the relative standard deviation value of the biosensor was 1.98% for 20 successive assays under the same conditions; this indicated that the proposed biosensor had a good operational stability.

Storage stability of the biosensor

To assess the storage stability of the proposed biosensor, measurements were periodically carried out

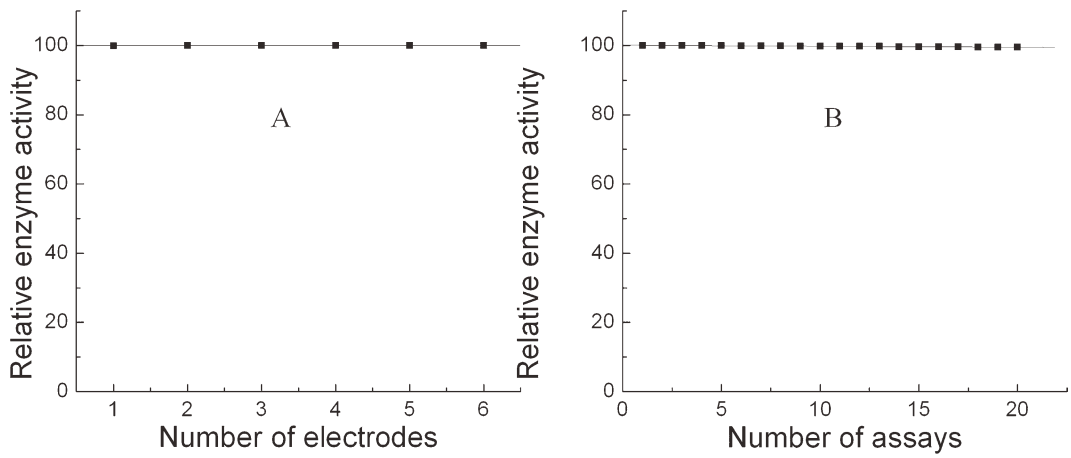

Figure 13 Operational stability of the PPy–MWCNT–AO biosensor.

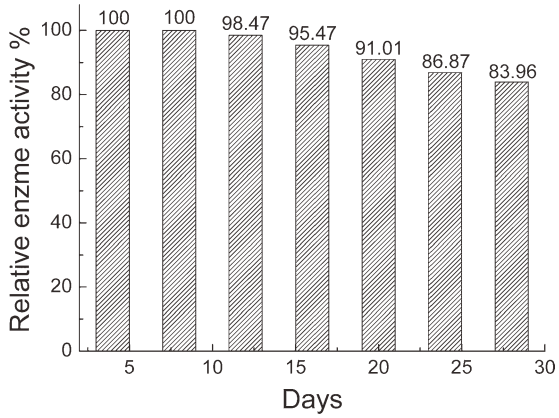

Figure 14 Storage stability of the PPy–MWCNT–AO biosensor.

every 4 days for 4 weeks in 0.05*M* PBS (pH 6.5) containing equal amounts of VC. As shown in Figure 14, no loss of relative enzyme activity was observed for 8 days, and the enzyme activity decreased approximately 1.53% after 12 days of storage. Moreover, 83.96% of the enzyme activity still remained even after 4 weeks of storage. There were two main reasons for this good stability of the proposed biosensor. First, the PPy–MWCNT composites were very stable on the surface of the electrode. Second, the PPy–MWCNT composites provide a biocompatible microenvironment for maintaining the relative enzyme activity and preventing its possible leakage from the surface of the electrode; this is very beneficial for the application of enzyme-based biosensors.

CONCLUSIONS

In conclusion, an amperometric VC biosensor was fabricated successfully with PPy–MWCNT composite films as the immobilized matrix of AO with a one-step electrodeposition technique. The proposed biosensor showed superior performance, including a wide linear range, fast current response, low detection limit, high bioaffinity, and good enzyme activity and good operational and storage stabilities. Hence, good performance of the proposed biosensor was beneficial for further applications in agriculture, and the PPy–MWCNT composites is also an interesting candidate for the design of biosensors. Moreover, the development of an AO-based biosensor for the detection of VC in vegetables, fruits, grain crops, agricultural food products, and beverages is also in progress.

References

1. Akyilmaz, E.; Dinckaya, E. Talanta 1999, 50, 87.
2. Lopes, P.; Drinkine, J.; Sacier, C.; Glories, Y. Anal Chim Acta 2006, 555, 242.
3. Hernandez, Y.; Lobo, M. G.; Gonzalez, M. Food Chem 2006, 96, 654.
4. Andreu, Y.; Marcos, S. D.; Castillo, J. R.; Galbán, J. Talanta 2005, 65, 1045.
5. Matsumoto, K.; Yamada, K.; Osajlma, Y. Anal Chem 1981, 53, 1974.
6. Stevanato, R.; Avigliano, L.; Finazzi-Agrò, A.; Rigo, A. Anal Biochem 1985, 149, 537.
7. Uchiyama, S.; Hasebe, Y.; Tanaka, M. Electroanalysis 1997, 9, 176.
8. Wang, H. Y.; Mu, S. L. J Electroanal Chem 1997, 436, 43.
9. Murata, K.; Nakamura, N.; Ohno, H. Electroanalysis 2007, 19, 530.
10. Wang, X. Y.; Watanabe, H.; Uchiyama, S. Talanta 2008, 74, 1681.
11. Sezgintürk, M. K.; Koca, H. B.; Özben, Y. S.; Dinçkaya, E. Artif Cells Blood Sub 2010, 38, 215.
12. Liu, M.; Wen, Y. P.; Xu, J. K.; He, H. H.; Li, D.; Yue, R. R.; Lu, B. Y.; Liu, G. D. Anal Sci 2011, 27, 477.
13. Liu, M.; Wen, Y. P.; Li, D.; Yue, R. R.; Xu, J. K.; He, H. H. Sensor Actuators B 2011, 159, 277.
14. Wang, J.; Xu, Y. L.; Chen, X.; Sun, X. F. Compos Sci Technol 2007, 67, 2981.
15. Lee, Y. K.; Lee, K. J.; Kim, D. S.; Lee, D. J.; Kim, J. Y. Synth Met 2010, 160, 814.
16. Ketpang, K.; Park, J. S. Synth Met 2010, 160, 1603.
17. Liu, Y. C.; Tsai, C. J. J Electroanal Chem 2002, 537, 165.
18. Liu, Y. C.; Tsai, C. J. Chem Mater 2003, 15, 320.
19. Deo, R. P.; Wang, J.; Block, I.; Mulchandani, A.; Joshi, K. A.; Trojanowicz, M.; Scholz, F.; Lin, Y. Anal Chim Acta 2005, 530, 185.
20. Cai, J.; Du, D. J Appl Electrochem 2008, 38, 1218.
21. Kumar, B.; Kumar, I.; Singh, R. P. Polym Compos 2009, 30, 855.
22. Spitalsky, Z.; Matejka, L.; Slouf, M.; Konyushenko, E. N.; Kovarova, J.; Zemek, J.; Kotek, J. Polym Compos 2009, 30, 1378.
23. Shahrokhian, S.; Asadian, E. J Electroanal Chem 2009, 636, 40.
24. Wan, Q. J.; Wang, X. W.; Yu, F.; Wang, X. X.; Yang, N. J. J Appl Electrochem 2009, 39, 785.
25. Sharma, R. K.; Karakoti, A.; Seal, S.; Zhai, L. J Power Sources 2010, 195, 1256.
26. Yang, S. L.; Qu, L. B.; Yang, R.; Yang, R.; Liu, C. J Appl Electrochem 2010, 40, 1372.
27. Jacobs, C. B.; Peairs, M. J.; Venton, B. J. Anal Chim Acta 2010, 662, 106.
28. Balavoine, F.; Schultz, P.; Richard, C.; Mallouh, V.; Ebbesen, T. W.; Mioskowski, C. Angew Chem Int Ed 1999, 38, 1912.
29. Lin, Y.; Lu, F.; Wang, J. Electroanalysis 2004, 16, 145.
30. Elie, A. G.; Lei, C.; Baughman, R. H. Nanotechnology 2002, 13, 559.
31. Sarma, A. K.; Vatsyayan, P.; Goswami, P.; Minteer, S. D. Biosens Bioelectron 2009, 24, 2318.
32. Davis, J. J.; Green, M. L. H.; Hill, H. A. O.; Leung, Y. C.; Sadler, P. J.; Sloan, J.; Xavier, A. V.; Tsang, S. C. Inorg Chim Acta 1998, 272, 265.
33. Luo, X.; Killard, A. J.; Morrin, A. Anal Chim Acta 2006, 575, 43.
34. Riggs, J. E.; Guo, Z.; Carroll, D. L.; Sun, Y. P. J Am Chem Soc 2000, 122, 5879.
35. Zengin, H.; Zhou, W.; Jin, J.; Czerw, R.; Smith, D. W., Jr.; Echegoyen, L.; Carroll, D. L.; Foulger, S. H.; Ballato, J. Adv Mater 2002, 14, 1480.
36. Wei, Z.; Wan, M.; Lin, T.; Dai, L. Adv Mater 2003, 15, 136.
37. Santhosh, P.; Gopalan, A.; Lee, K. P. J Catal 2006, 238, 178.
38. Arami, H.; Mazloumi, M.; Khalifehzadeh, R.; Sadrnezhaad, S. K. Mater Lett 2007, 61, 4412.
39. Peng, C.; Ji, J.; Chen, G. Z. Electrochim Acta 2007, 53, 529.

40. Deng, J.; Peng, Y.; He, C.; Long, X. P.; Li, P.; Chan, A. S. C. Polym Int 2003, 52, 1185.
41. Sahoo, N. G.; Jung, Y. C.; So, H. H.; Cho, J. W. Synth Met 2007, 157, 376.
42. Karim, M. R.; Lee, C. J.; Chowdhury, A. M. S.; Nahar, N.; Lee, M. S. Mater Lett 2007, 61, 1690.
43. Park, J. H.; Ko, J. M.; Park, O. O.; Kim, D. W. J Power Sources 2002, 105, 24.
44. Xu, Y.; Jiang, Y.; Cai, H.; He, P. G.; Fang, Y. Z. Anal Chim Acta 2004, 516, 24.
45. Sabatani, E.; Cohen-Boulakia, J.; Bruening, M.; Rubinstein, I. Langmuir 1993, 9, 2978.
46. Lien, T. T. N.; Lam, T. D.; An, V. T. H.; Hoang, T. V.; Quang, D. T.; Khieu, D. Q.; Tsukahara, T.; Lee, Y. H.; Kim, J. S. Talanta 2010, 80, 1167.
47. Nakamura, T.; Makino, N.; Ogura, Y. J Biochem 1968, 64, 194.
48. Alaejos, M. S.; Montelongo, F. J. G. Chem Rev 2004, 104, 3244.
49. Wang, G.; Xu, J. J.; Chen, H. Y.; Lu, Z. H. Biosens Bioelectron 2003, 18, 340.
50. Tan, X. C.; Li, M. J.; Cai, P. X.; Luo, L. J.; Zou, X. Y. Anal Biochem 2005, 337, 117.
51. Su, C. M.; Puls, R. W. Environ Sci Technol 1999, 33, 165.
52. Barnett, S. J.; Soutsos, M. N.; Millard, S. G.; Bungey, J. H. Cem Concr Res 2006, 36, 439.